

A Torsional Balance that Resolves Sub-micro-Newton Forces

Manuel Gamero-Castaño and Vlad Hruby
Busek Co. Inc.
11 Tech Circle
Natick, MA 01760-1023
busek@busek.com
508-655-5565

Manuel Martínez-Sánchez
Massachusetts Institute of Technology
77 Massachusetts Ave, 37-401
Cambridge, MA 02139

IEPC-01-235

In this article we present our ongoing research on micro-Newton thrust stands. The capability of measuring thrust in the range of micro-Newtons is essential to validate the performance of devices such as colloid thrusters and FEEPs. Although time of flight and energy analysis techniques have been satisfactory to measure the thrust and the specific impulse associated with colloid beams, it is clear that the confidence level in a micro-Newton thruster would increase by the direct thrust measurement provided by a thrust stand. Our approach is based on a torsional balance. Key features include the use of a fiber optic displacement sensor for measuring the angular displacement of the balance's arm, the use of electrostatic forces to calibrate accurately applied torque and balance's response, and an external damping mechanism. We measured comfortably thrust values as low as 0.11 μN , which were generated with a single emitter colloid source. A rough measurement of the resolution of this torsional balance yields a value of 0.01 μN , and we expect to lower this figure with further improvements.

1.0 Introduction

The needs for micropropulsion are of two kinds. First, there is a need for efficient primary thrusters for satellites with mass lower than about 20 Kg. For many missions, studies^{1,2} have shown that it is not the payload, but the “ancillary” systems, primarily the propulsion system, that limit miniaturization.

This point may have been overlooked in some of the early micro-satellite literature, which emphasized the seemingly unbounded potential for miniaturization of electronics and sensors alone. But, of course, the ΔV requirements for a satellite are largely mission, and not size dependent (and in some cases, like drag compensation, they increase as size decreases). Second, high precision microthrusters are needed for a variety of scientific missions such as the Laser Interferometer Space Antenna (LISA), Earth Science Experimental Mission 5 (EX-5), and Laser Interplanetary Ranging Experiment (LIRE). The requirements on the micropropulsion system can be

Copyright © by M. Gamero-Castaño. Published by the Electric Rocket Propulsion Society with permission.
Presented as Paper IEPC-01-235 at the 27th International Electric Propulsion Conference, Pasadena, CA, 15-19 October, 2001

most stringent. For example, the Disturbance Reduction System (DRS), a technology demonstration project within the New Millennium Program aimed to develop and test some of the technologies required by these scientific missions, calls for thrusters capable of delivering continuously thrust in the range $1 \mu\text{N} - 20 \mu\text{N}$, with a resolution of $0.1 \mu\text{N}$ and a specific impulse of at least 500 s. Although thrusters with these performance parameters have not been qualified yet, it is recognized that Field Emission Electric Propulsion (FEEP) and Colloid thrusters are the most promising candidates.³

A challenging issue associated with micropropulsion is the accurate validation of performance. Thrust levels and noise, specific impulse and thrusting efficiency are some of the parameters that define a thruster. Measuring them when the thrust is of the order of $1 \mu\text{N}$ or smaller is not a trivial matter. So far, the performance of FEEPs operating at this level had been inferred from correlations relating their beam current and acceleration voltage with the delivered thrust. Recently, Genovese et al. used a thrust stand to measure the thrust yielded by a FEEP prototype in the micro-Newton range.⁴ The correlation-approach can be used for Colloid thrusters as well, although a more precise method (time of flight) based on the measurements of the velocity and mass flow rate of the beam has been traditionally used.^{5,6} In any case, it is apparent that thrust stands with enough sensitivity need to be developed. Boccaletto & d'Agostino indicate that torsional balances are the most effective way of measuring forces in the micro-Newton level.⁷ Other concepts such as capacitive and pendulum balances are handicapped by the total weight they can support or the disturbing effect caused by external vibration noise.

Our interest in micropropulsion, and more specifically in colloid thrusters, has triggered our research in very sensitive torsional balances. In this article we describe the design and testing of one of such device. We will prove that a non optimized version of this thrust stand has an approximate resolution of $0.01 \mu\text{N}$, while being able to support a load of the order of 2 kg. Also, we report initial measurements of the thrust associated with a single colloid beam.

2.0 Description of the Torsional Balance and Experimental Facility

A photograph of the torsional balance is shown in figure 1. A symmetric aluminum arm, with a colloid source in one of its ends, is fixed to the balance frame by means of two flexural pivots (Lucas Aerospace, Utica NY). Each pivot has a nominal torsional spring rate of $1.60 \times 10^{-3} \text{ Nm/degree}$, and can hold an axial load of up to 20.0 N. The motion of the arm is constrained by the pivots to rotation only. The original design also included two stepping motors in the frame base aimed to control its inclination, although they were not used in these preliminary experiments. As a reference, the length and height of the arm are 48 cm and 22 cm respectively. The linear displacement of the arm, resulting from a given excitation, is measured with a fiber optic displacement sensor (Philtex, Inc. PO Box 359 Arnold, MD 21012). Its resolution is 5.0 nm in the DC-100 Hz range, dropping to $0.15 \mu\text{m}$ at a frequency of 200 kHz. Other features observed in this figure such as an electrospray source with power and liquid feed lines, calibration electrodes and a damping circuit will be described in following paragraphs.

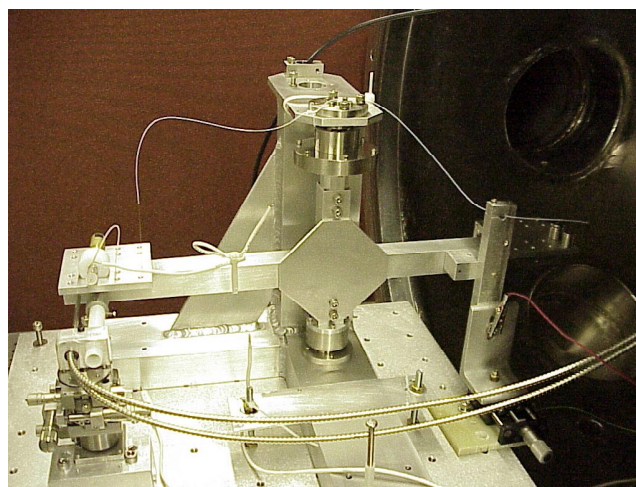


Figure 1 Torsional balance placed in vacuum facility

The usefulness of the balance rests on knowing precisely the dependence between the balance's displacement and the torque that causes it. Clearly,

the calibration of the balance involves the use of a test force, which has to be accurately varied in the range of micro-Newtons. Because of the minute values of the torque to be measured, it seems reasonable that the test force will have to act at “a distance”, with no physical contact between the balance arm and the arrangement used to apply the force. Furthermore, because of geometric constraints and the values required, it seems that only magnetic and electrostatic forces will be appropriate for our purpose.

We used the electrostatic force between two charged electrodes as a calibration standard. The negative pressure P exerted by an electric field on the surface of a conductor is given by:⁸

$$P = \frac{1}{2} \epsilon_0 E^2 \quad [1]$$

where E is the electric field on the surface of the electrode (E is always normal to its surface), and ϵ_0 is the permittivity of the vacuum. Thus, for the simple case in which a voltage difference V is set between two plane electrodes of area A and separated by a gap L , the electrodes will attract each other with a force of magnitude:

$$F = \frac{1}{2} \epsilon_0 \left(\frac{V}{L} \right)^2 A \quad [2]$$

As a reference, the attracting force for typical values of $V = 100$ Volts and $L = 1$ mm, is $4.427 \mu\text{N}$ per square centimeter. The actual calibration electrodes, along with the linear displacement sensor, are shown in figure 2. A base of a cylindrical electrode with a diameter and a height of 12 mm and 13 mm, is fixed to one side of the balance’s arm, at 21 cm from its axes. A second larger electrode, physically isolated from the balance, faces it. The relative position between the two electrodes can be varied with an XYZ positioning stage. The actual gap between electrodes (1.56 mm for the experiments reported below) can be accurately inferred from a measurement of the linear displacement sensor.

Let us demonstrate with a simple experiment the accuracy of Eq. [2], since we will use this formula to estimate the force between the calibration electrodes. We placed the smaller electrode on a precision

balance (resolution of 0.1 mg, or equivalently $0.98 \mu\text{N}$), as shown in figure 3. This electrode was grounded using a thin copper wire to prevent spurious torques. The larger electrode was positioned on top, and connected to the positive output of a power supply. The gap between electrodes could be adjusted with a positioner.

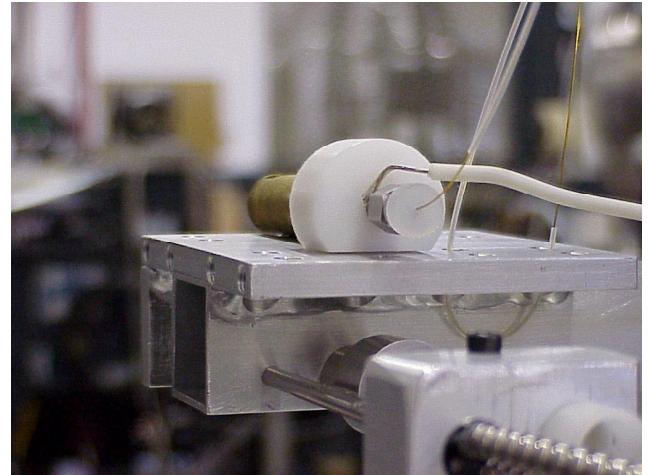


Figure 2. Detail of the calibration electrodes and linear displacement sensor. An electro spray source is also mounted on the balance.

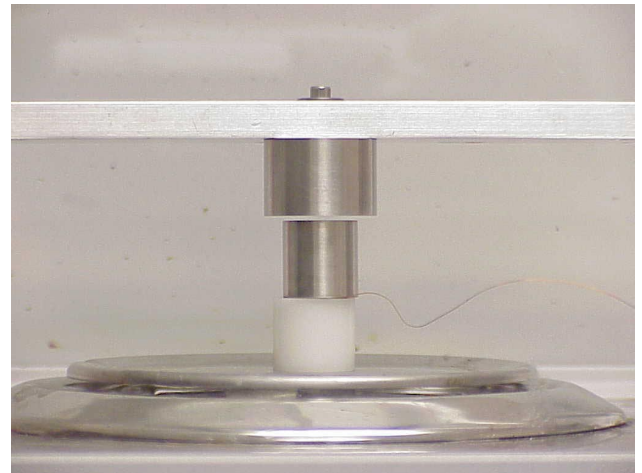


Figure 3. The calibration electrodes are mounted on a laboratory balance to test the accuracy of Eq. [2]

With this arrangement we could compare the actual lifting force acting on the small electrode, with the expected electrostatic force (the area of the small electrode is the appropriate value of A in (2)). This comparison, for two different gap distances, is given in figure 4. Note the linearity of the data and the negligible values of the intersections with the vertical axis. Ideally the slopes of these straight

lines would be identically one. However, the slopes have larger values due to the importance of end effects. This is more evident for the larger gap, as it should be. For the 3.02 mm gap, the error is $\sim 42\%$, while for the 1.03 mm gap the error is reduced to a reasonable $\sim 10\%$. We conclude that Eq. [2] approximates the calibration force reasonably well, although we will have to compute eventually a more accurate relation between force, voltage difference and gap (e.g. solving numerically Laplace equation for the electric potential field)

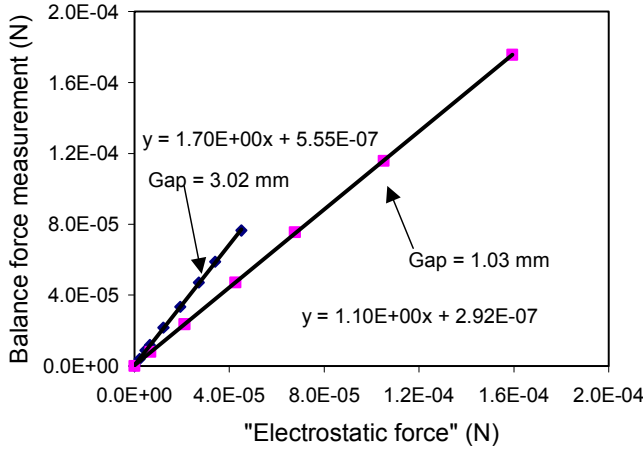


Figure 4. Comparison between electrostatic force (approximated by [2]) and the lifting force measured by a laboratory balance.

From elementary mechanics we know that the dynamics of the arm is correctly described by a second order differential equation in which the angular acceleration of the arm is proportional to the sum of the exciting torque, a torque proportional to the angular displacement, and a second torque proportional to the angular velocity:

$$\ddot{\vartheta} + \frac{\lambda}{I} \dot{\vartheta} + \frac{\kappa}{I} \vartheta = \frac{1}{I} L(t) \quad [3]$$

where I is the moment of inertia of the arm about the axis of rotation, and λ and κ are damping and torsional spring rate constants of the flexural pivots. $L(t)$ is the torque applied to the balance, which is a function of time. The ratio $4\kappa I/\lambda^2$ largely determines the motion of the balance. Thus, for large values of this ratio, any excitation (e. g. a torque in the form of a step) will make ϑ oscillate at the natural frequency of the balance, $\omega_s = \frac{1}{4\pi I} \sqrt{4\kappa I - \lambda^2}$, with an amplitude that decreases exponentially in time,

$Exp\left[-\frac{1}{2} \frac{\lambda}{I} t\right]$, until a steady state is reached (of course, the exciting torque must reach a steady state as well). This is known as weak damping, as opposed to the case of strong damping ($4\kappa I/\lambda^2 < 1$) in which the motion of the arm reaches its steady state without undergoing any oscillation. It turns out that a system strongly damped is most convenient. The reasons behind this are clear: in a weakly damped system, any undesirable mechanical noise upsets the steady state of the balance forcing it to oscillate. In practice, it takes too long for these oscillations to be eliminated, making the measurement of minute torques difficult. Unfortunately, there are not springs that at the same time are very sensitive (large κ) and able to dissipate energy fast (large λ). To solve this problem one has to implement an external damping circuit, an arrangement that is able to apply a torque proportional to the angular velocity of the balance arm. The actuator of our damping circuit can be seen in figure 1, in the form of an electrode facing the right side of the balance's arm. The voltage of this electrode (and thus the torque applied to the arm) is determined by an electronic circuit that takes the displacement of the arm as an input, computes its derivative, and generates a positive high voltage (approximately 100 V) signal proportional to it. Notice that the damping torque applied to the arm is not proportional to $\dot{\vartheta}$, but to $\dot{\vartheta}^2$ instead. However, we can always set the working point of the electrode at say 100 V, and consider only small variations of the electrode voltage around this offset value. Thus, within this linearized range, the damping torque is conveniently linear in $\dot{\vartheta}$.

The thrust stand has been tested in the vacuum facility shown in figure 5. A cylindrical chamber with a diameter of 0.66 m and a length of 0.77 m is evacuated with a turbomolecular pump (250 l/s) backed by a two-stage mechanical pump (1.2 l/s). The base pressure of the facility is 10^{-6} torr. The chamber rests on an optical bench, although its isolation capability was never activated. The thrust stand itself is placed on a tray fixed to a sliding door of the chamber. An electrospray source with a single emitter rests on the left side of the balance's arm, and its thrust was measured. The basic elements of the source are an electrospray needle and a facing

extractor. The extractor is the cylindrical part made of brass observed in figure 6. The electro spray needle is inside the extractor, aligned with its axis. A small orifice drilled through the end of the extractor allows the passage of the whole electro spray emitted from the tip of the needle. In order to set an electro spray, a liquid flow rate must be fed to the tip of the needle and an appropriate voltage difference has to be established between needle and extractor. A high voltage line connects the electro spray needle with a power supply outside the vacuum chamber (the extractor is grounded by direct contact with the balance arm), and a teflon line is used to feed the liquid solution required by the electro spray. These two lines are designed in such a way as to introduce negligible torques into the balance's arm. The connections and feedthroughs needed for these lines, as well as for others, were implemented in the multiple ports of the chamber.

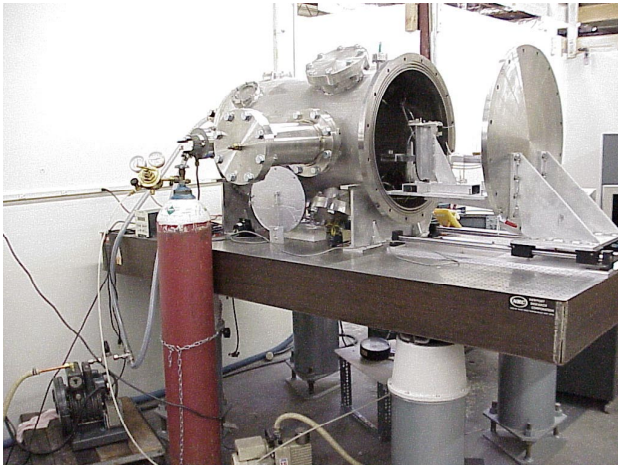


Figure 5. Vacuum facility used to test the balance

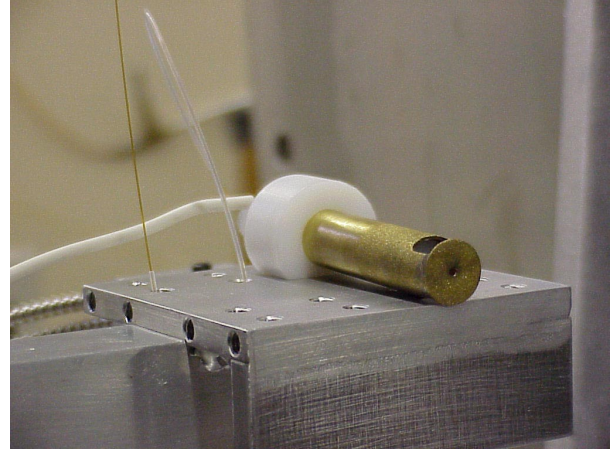


Figure 6. Electro spray source. The thrust associated with its colloid beams is measured with the thrust stand

3.0 Experimental Results and Discussion

Figure 7 shows the response of the balance to an excitation in the form of a torque of $0.734 \mu\text{Nm}$ ($3.49 \mu\text{N}$ at 0.21 m from the axis), and which is applied during 0.54 seconds. The response of the balance is given as the output of the linear displacement sensor. The torque is induced with the calibration electrodes. The external damping circuit is not operative. The torque is applied at $t = 5.8 \text{ s}$, causing the balance to go into oscillations. The natural frequency of the balance is readily obtained from this figure, $\omega_s = 0.448 \text{ Hz}$. Also, it is observed that the motion evolves towards its steady state very slowly. Beside this qualitative information, the data in figure 7 can be used to estimate the parameters I and λ of the system (κ can be obtained from a static calibration of the balance, $\kappa = 7.43 \times 10^4 \mu\text{Nm}$, or equivalently $\kappa = 1.30 \times 10^{-3} \text{ Nm/degree}$). Thus, the natural frequency is simply $\frac{1}{4\pi I} \sqrt{4\kappa I - \lambda^2}$, while

the speed at which the arm is damped yields the time constant λ/I ($3.05 \times 10^{-3} \text{ s}^{-1}$). Using the torsional spring rate and these expressions we obtain the values of $2.86 \times 10^{-5} \text{ kgm}^2\text{s}^{-1}$ and $9.37 \times 10^{-3} \text{ kgm}^2$ for λ and I respectively.

The improvement associated with the use of the damping circuit is shown in figure 8, where we plot both the torque and the associated response of the balance. Notice that the balance's arm reaches its steady state much faster than before. Also, the output of the displacement sensor is quite steady, insensitive to excitations associated with background noise.

The calibration of the balance is exemplified in figures 9 and 10. The usual procedure is to increase the voltage difference between the calibration electrodes through a series of steps, and record how the output of the displacement sensor varies. Because we have a good estimate for the correspondence between electrode voltage and applied force, Eq. [2], the desired relation between

linear displacement output and calibration force is readily obtained. From the linear fitting of data in figure 10, we get a value of $\Delta\text{LDS}/\Delta F$ of $0.123 \text{ V}/\mu\text{N}$. Notice that the calibration in figure 10 focuses on the submicro-Newton range, which is the one of interest in our experiments. A calibration for a higher range can be obtained without any problem.

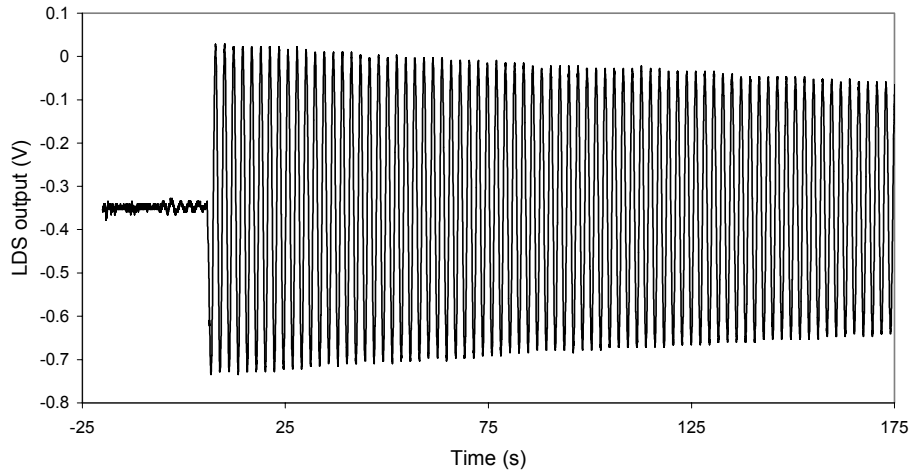


Figure 7. Response of the balance to a short excitation. The motion is not damped externally

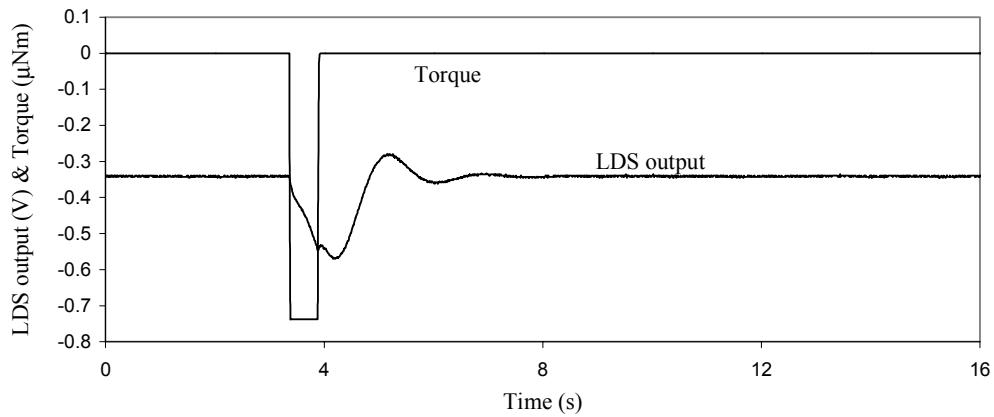


Figure 8. Response of the balance to a short excitation. The balance is actively damped

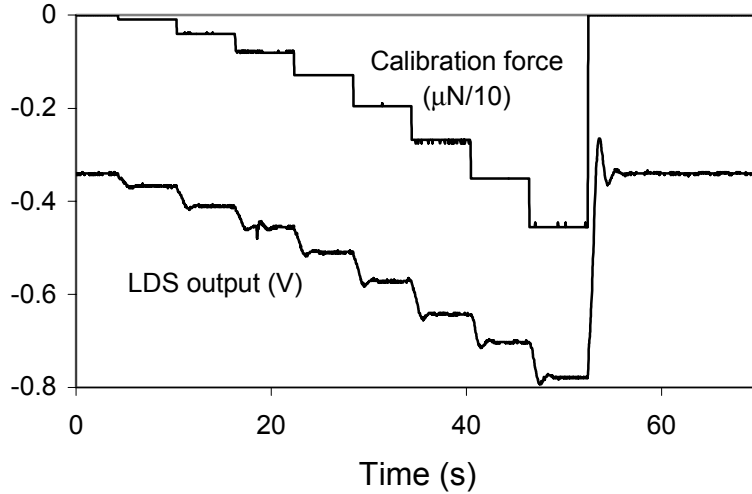


Figure 9. Response of the balance to a series of steps of the calibration force

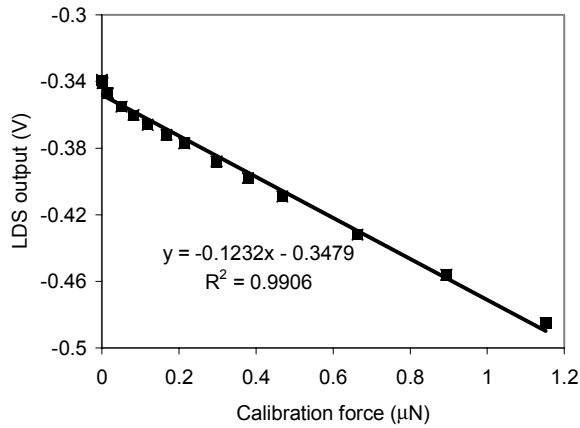


Figure 10. Calibration of LDS output versus force.

The measurements of the thrust generated by the single electro spray source are shown in figures 11a,b,c,d,e. We electro sprayed a solution of the liquid tributyl phosphate having a relatively low electrical conductivity. We did not measure relevant parameters such as the liquid flow rate or the electrical conductivity in the initial experiments reported here. In all cases the voltage difference between the electro spray needle and the grounded extractor is kept constant and equal 1531 V. The acceleration voltage of the beam is this value minus a voltage drop (of the order of 250 V for this solution) associated with the formation of the electro spray.⁶ The electro spray is turned on and off by allowing or interrupting the feed of liquid to the electro spray needle. The different spectra in figures 11 show the thrust associated with different electro spray currents, or equivalently with different flow rates (the electric current is roughly

proportional to the square root of the flow rate⁹). The output of the balance begins to be recorded when the electro spray is turned off. Then, the electro spray is turned on and its flow rate kept constant, which translates to a step of the thrust measured by the balance. Finally, we stop taking data while the electro spray is on. These figures demonstrate that the torsional balance can measure the performance of actual colloid thrusters in the micro-Newton and submicro-Newton range, which was generally believed to be a most difficult task. Figure 11e shows the complete cycle in which the thruster is off, turned on and off again. It is observed that, under appropriate conditions, the shift of the equilibrium position of the balance can be made quite small. This is important because it simplifies the analysis of measurements taken over long periods of time.

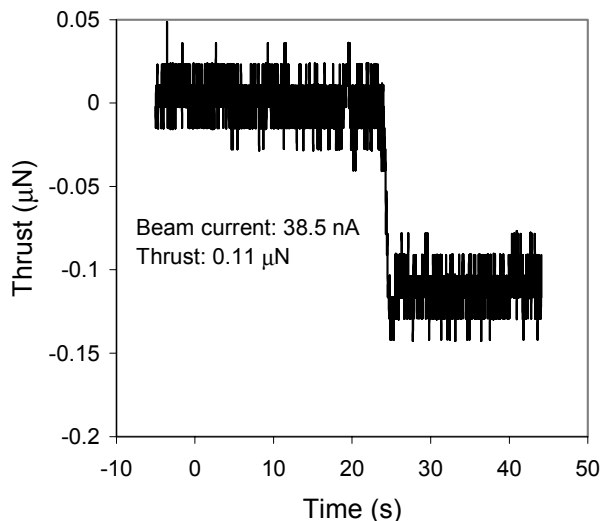


Figure 11a. Thrust measured by the torsional balance. The step of the curve is triggered by turning on an electrospray source. The beam current and thrust are 38.5 nA and 0.11 μN

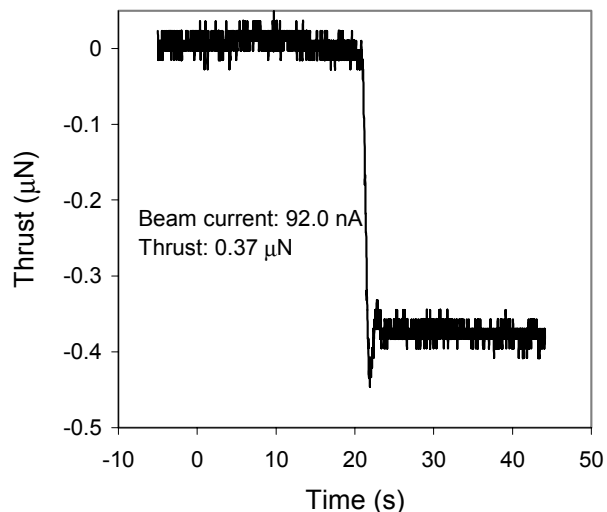


Figure 11c. Thrust measured by the torsional balance. The beam current and thrust are 92.0 nA and 0.37 μN

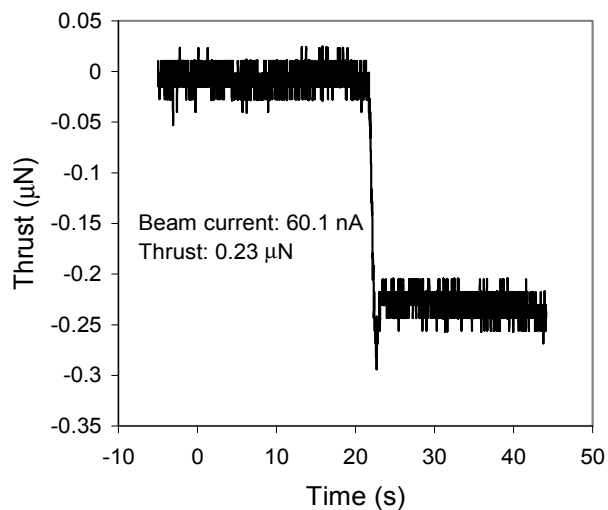


Figure 11b. Thrust measured by the torsional balance. The beam current and thrust are 60.1 nA and 0.23 μN

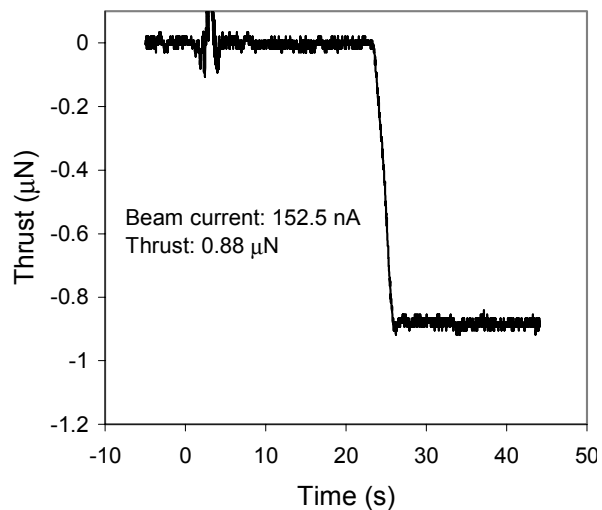


Figure 11d. Thrust measured by the torsional balance. The beam current and thrust are 152.5 nA and 0.88 μN

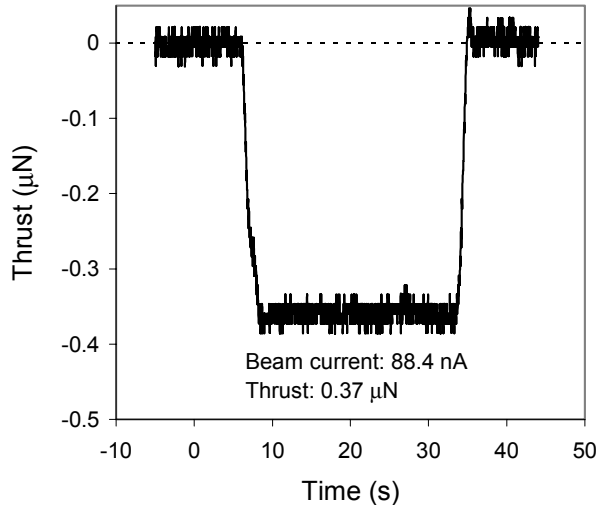


Figure 11e. Thrust measured by the torsional balance. The electro spray is initially off, then it is turned on during approximately 25 s, and turned off again.

An important issue is the resolution with which the torsional balance can measure thrust. Although in this preliminary report we will not undertake a rigorous analysis of the balance resolution, and how it depends on the excitation frequency, it is worth to compute a rough estimate. To do so let us use the data in any of figures 11, e.g. the balance output associated with $I = 60.1$ nA when the thruster is off. The standard deviation of this data, which gives a first estimate of the resolution of the balance, is $0.011 \mu\text{N}$. Still, notice that this value is deceiving in the sense that most of the noise in figure 11b is actually due to 60 Hz electronic noise, which could (and should) be filtered out by either data analysis or electronic means. The actual resolution of the balance will depend on the exciting frequency and in general will be, for the frequencies of interest, smaller than $0.01 \mu\text{N}$. To have a better idea of the resolution we could do the following: first, estimate (e.g. using FFT techniques) the power spectrum of the balance output in the absence of any excitation. Second, measure the frequency response of the balance. Finally, we would have to weigh the power spectrum of the balance signal using the response frequency of the balance. The results of this exercise will be reported elsewhere.

4.0 Conclusions

In this article we described the initial tests of a torsional balance that can measure forces in the sub-micro-Newton range. This type of diagnostic tool is essential to characterize the performance of micro-Newton thrusters such as FEEPs and Colloid thrusters. These propulsion concepts are expected to enable both the proliferation of very small spacecraft, and several scientific missions.

We could measure thrust values as low as $0.11 \mu\text{N}$, and proved that the resolution of the balance at low frequencies (less than approximately 0.5 Hz) is much smaller than $0.01 \mu\text{N}$. We advance that future research will be focused on the optimization of the resolution, the study of the effect of different loads on the balance performance, and the comparison of thrust measurements of colloid beams obtained with both the time of flight technique and this thrust stand.

Acknowledgement

This research is supported by a NASA Phase II SBIR contract. We acknowledge gratefully the support given by J. Sovey, the NASA technical monitor of this contract.

References

1. J. Mueller. "Thruster Options for Microspacecraft: A Review and Evaluation of Existing Hardware and Emerging Technologies", 33rd AIAA/ASME/SAE/ASEE Joint Propulsion Conference, Seattle, Washington (1997).
2. R. Fleeter. "Microspacecraft". The Edge City Press, Reston, Virginia (1995).
3. J. Reichbach, R. Sedwick & M. Martínez-Sánchez. "Micropropulsion System Selection for Precision Formation-Flying Satellites". Paper AIAA-2001-3646, 37th Joint Propulsion Conference, Salt Lake City, UT (2001).
4. A. Genovese, W. Steiger & M. Tajmar. "Indium FEEP Microthruster: Experimental Characterization in the 1-100 μN Range". Paper AIAA 2001-3788, 37th Joint Propulsion Conference, Salt Lake City, UT (2001).
5. R. E. Hunter & S. H. Wineland. "Charged Colloid Generation Research", Space Electronics Symposium, Los Angeles, CA (1965).

6. M. Gamero-Castaño & V. Hruby. “Electrospray as a Source of Nanoparticles for Efficient Colloid Thrusters”, *J. of Propulsion and Power* 17, 977-987 (2001)
7. L. Boccaletto & L. d’Agostino. “Design and Testing of a Micro-Newton Thrust Stand for FEEP”. Paper AIAA 2000-3268, 36th Joint Propulsion Conference, Huntsville, AL (2000).
8. L. D. Landau & E. M. Lifshitz. “Electrodinámica de los Medios Continuos” Editorial Reverté, Barcelona 36-40 (1975)
9. J. Fernández de la Mora & I. G. Loscertales. “The Current Emitted by Highly Conducting Taylor Cones”. *J. Fluid Mech.* 260, 155-184 (1994).